

Reinvestigation of the Photocyclization of 1,4-Phenylene Bis(phenylmaleic anhydride): Preparation and Structure of [5]Helicene 5,6:9,10-Dianhydride

Aryeh A. Frimer,^{*,†} James D. Kinder,[‡] Wiley J. Youngs,[§] and Mary Ann B. Meador

Polymer Branch, NASA Lewis Research Center, Cleveland, Ohio 44135, and The Ethel and David Resnick Chair in Active Oxygen Chemistry, Department of Chemistry, Bar-Ilan University, Ramat Gan 52900, Israel

Received November 22, 1994[®]

The I₂-catalyzed photooxidative cyclization of 1,4-phenylene bis(phenylmaleic anhydride) [PPMA] yields two products in an overall yield approaching 80%. Contrary to a previous report, the major product has been identified by X-ray crystallography as the novel [5]helicene-5,6,9,10-tetracarboxylic 5,6:9,10-dianhydride [HLDA], while the minor product (<5% yield) is the isomeric dibenz[*ah*]anthracene-5,6,12,13-tetracarboxylic 5,6:12,13-dianhydride [DBAA]. Partial irradiation permits the isolation of the monocyclization intermediate PMPA, which under the photolysis conditions generates the observed dicyclization products. Unlike HLDA, DBAA resists prolonged methanolysis to the corresponding acid esters. This confirms molecular modeling predictions that the 1,6-interaction between the H-4, H-7, H-11, and H-14 aromatic hydrogens and the corresponding neighboring carbonyl oxygens in DBAA inhibit opening of the resulting O–CO anhydride bond. Noteworthy as well is that HLDA, unlike the parent [5]helicene, resists further photocyclization under the reaction conditions to the corresponding benzo[*ghi*]perylene. AM1 semiempirical calculations indicate that, contrary to [5]helicene, there is no buildup of bonding interaction between the designated bonding carbons (C-1 and C-14) as one goes from the HOMO to the corresponding LUMO.

One of the highest priorities of the aerospace industry is the development of high-performance, low-density polymers and polymer matrix composites to serve as metal replacements.^{1,2} Over the past two decades,³ endcap-cross-linked polyimides have proven themselves to be among the best materials for these high temperature applications, combining stability, processibility, and good mechanical properties. Multifaceted and interdisciplinary research continues to improve both the thermo-oxidative stability and performance of these organic materials.^{4–7}

Our own research focus in this area^{8–10} has been in improving thermooxidative stability of the polyimide

system as a whole by stabilizing the most thermally labile bond therein, presumably the nitrogen–carbon bond of the >NC=O moiety. The dissociation energy of the latter is reported to be somewhere around 65 kcal/mol¹¹ or perhaps even as low as a mere 50 kcal/mol.¹² In light of this, our attention was drawn to work by Fields and colleagues^{13–15} who reported in this journal¹⁵ that I₂-catalyzed photooxidative cyclization¹⁶ (*vide infra*) of the new dianhydride 1,4-phenylene bis(phenylmaleic anhydride) [PPMA] yields the corresponding fully cyclized analog, dibenz[*ah*]anthracene-5,6,12,13-tetracarboxylic 5,6:12,13-dianhydride (DBAA, eq 1).

We noted that in the polyaromatic compound DBAA, the 1,6-interaction between the H-4, H-7, H-11, and H-14 aromatic hydrogens and the corresponding neighboring carbonyl oxygens are expected to inhibit opening of the resulting imide ring (eq 1). H-7 and H-14 are also

* Address correspondence to this author at Bar Ilan University. Tel.: 972-3-5318610. Fax: 972-3-5351250. E-mail: f66235%barilan.bitnet@vm.tau.ac.il.

† NRC-NASA Lewis Senior Research Associate, 1990–1995.

‡ NRC-NASA Lewis Research Associate, 1992–1995.

§ Department of Chemistry, The University of Akron, Akron, OH.

® Abstract published in *Advance ACS Abstracts*, February 15, 1995.

(1) Cassidy, P. E. *Thermally Stable Polymers*; Marcel Dekker: New York, 1980.

(2) See the collection of papers in: *Resins for Aerospace*; ACS Symposium Series No. 132; American Chemical Society: Washington DC, 1980.

(3) Serafini, T. T.; Delvigs, P.; Lightsey, G. R. *J. Appl. Polym. Sci.* **1972**, *16*, 905–915.

(4) Meador, M. A.; Cavano, P. J.; Malarik, D. C. In *Structural Composites: Design and Processing Technologies*; Proceedings of the Sixth Annual ASM/ESD Advanced Composites Conference, Detroit, MI, 8–11 Oct 1990; pp 529–539.

(5) Serafini, T. T.; Vannucci, R. D.; Alston, W. B. *Second Generation PMR Polyimides*, NASA TM X-71894.

(6) Vannucci, R. D.; Malarik, D. C.; Papadopoulos, D. S.; Waters, J. F. *Advanced Materials: Looking Ahead to the 21st Century*. Proceedings of the 22nd International SAMPE Technical Conference, Boston, MA, Nov 6–8, 1990, pp 175–185. Also NASA TM 103233.

(7) Bowles, K. *Materials-Process: The Intercept Point*. Proceedings of the 20th International SAMPE Technical Conference, Minneapolis, MN, Sep 27–29, 1988, pp 552–561. Also NASA TM 100922.

(8) Frimer, A. A.; Cavano, P. J. In *Polyimides: Materials, Characterization and Application*. Proceedings of The Fourth International Conference on Polyimides, Feger, C., Ed.; Society of Plastic Engineers, 1991, pp 17–20. Also NASA Technical Memorandum 105335, pp 1–5 (1991).

(9) (a) Frimer, A. A.; Cavano, P. J. In *HITEMP Review 1991: Advanced High Temperature Engine Materials Technology Program*; Gray, H. R., Ginty, C. A., Eds.; NASA CP-10082, 1991; pp 12-1–12-13. (b) Frimer, A. A.; Cavano, P. J.; Alston W. B.; Serrano, A. In *HITEMP Review 1992: Advanced High Temperature Engine Materials Technology Program, Volume I: Overviews, Fan/Compressor Materials (Polymer Matrix Composites), and Fibers*; Gray, H. R., Ginty, C. A., Eds.; NASA Conference Publication 10104, 1992; pp 14-1–14-15. In this latter paper, the correct identity of the major PPMA photocyclization product had not yet been determined. As a result it was thought to be DBAA, when in fact it is HLDA (*vide infra*).

(10) Frimer, A. A.; Cavano, P. J. In *Advances in Polyimide Science and Technology*; Feger, C., Ed.; Technomic Publishing Co.: Lancaster, PA, 1993; pp 41–54.

(11) Jellinek, H. H. G.; Dunkle, S. R. In *Degradation and Stabilization of Polymers*; Jellinek, H. H. G., Ed.; Elsevier: New York, 1983; pp 66–161. See especially pp 75, 77, and 103ff.

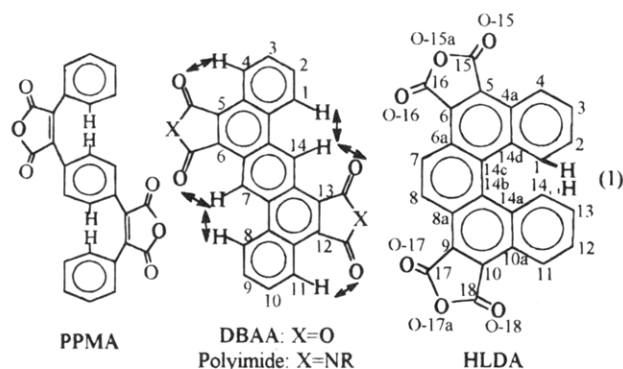
(12) Ranby, B.; Rabeck, J. F. *Photodegradation, Photo-oxidation and Photostabilization of Polymers*; Wiley: New York, 1975; p 236.

(13) Fields, E. K.; Winzenberg, M. L.; Behrend, S. J. *Disubstituted Maleic Anhydrides*, U. S. Patent no. 4596367, June 24, 1986.

(14) Fields, E. K.; Winzenberg, M. L.; Behrend, S. J. *Disubstituted Maleic Anhydrides*, U. S. Patent no. 4638072, Jan 20, 1987.

(15) Fields, E. K.; Behrend, S. J.; Meyerson, S.; Winzenberg, M. L.; Ortega, B. R.; Hall, H. K., Jr. *J. Org. Chem.* **1990**, *55*, 5165–5170.

(16) Mallory, F. B.; Mallory, C. W. *Org. React.* **1984**, *30*, 1–456.

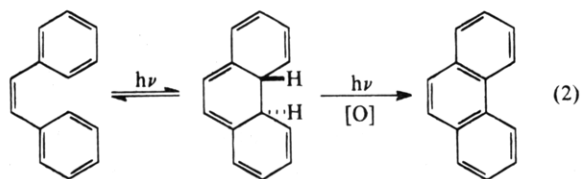


expected to feel further steric pressure from H-1 and H-8, which would further counter any opening or stretching of the imide N–CO bond. We hoped that this combined buttressing effect would serve to improve the TOS of polyimides derived therefrom. Our structural predictions agreed with molecular modeling studies.¹⁷ These indicated that DBAA should be an essentially planar and rigid molecule (Figure 1); nevertheless, H-14 and H-7 are slightly twisted away from the carbonyl,¹⁸ reflecting the aforementioned 1,6-interactions.

As reported below, our reinvestigation of the photolysis of PPMA has led us to the conclusion that Fields and coworkers^{13–15} erred in identifying DBAA as the major product of this reaction. While DBAA is formed in low yield, the main product of the photolysis is the isomeric [5]helicene-5,6,9,10-tetracarboxylic 5,6:9,10-dianhydride [HLDA] (eq 1). The preparation and characterization of this novel helicene dianhydride is described herein.

Results And Discussion

A. Photooxidative Cyclization of PPMA. *cis*-Stilbene moieties are known to undergo a reversible photocyclization to the corresponding *trans*-4a,4b-dihydrophenanthrene. The latter can be oxidized to the corresponding phenanthrene by hydrogen acceptors such as iodine and/or oxygen (eq 2). In systems where more



than one stilbene moiety is present, two consecutive cyclizations can occur.¹⁹

Fields reports that PPMA, which contains two such stilbene systems, undergoes this double transformation, yielding yellow powder in a 25–30% yield.^{13–15} We have found that this yield can be raised to as much as 88%, when the Katz propylene oxide modification is utilized

(17) Autodesk HyperChem 3, AM1 semiempirical calculation; results were confirmed in several substrates by related calculations using Tripos Sybyl 5.4 Molecular Modeling Program.

(18) The calculated heat of formation of the geometry-optimized DBAA is -80.968 kcal/mol (gradient 0.036 kcal/mol/Å) as compared to a value of -46.631 (gradient 20.112) for the completely flat analog. The HyperChem geometry optimization introduces a slight twist throughout the ring system so that the H-7 hydrogen is bent down below the ring plane while H-8 and the carbonyl are bent up creating a dihedral angle of ca. 0.035° in each case. The dihedral angle between H-7 and H-14 is ca. 0.32° .

(19) Mallory, F. B.; Mallory, C. W. *Org. React.* **1984**, *30*, 1–456.

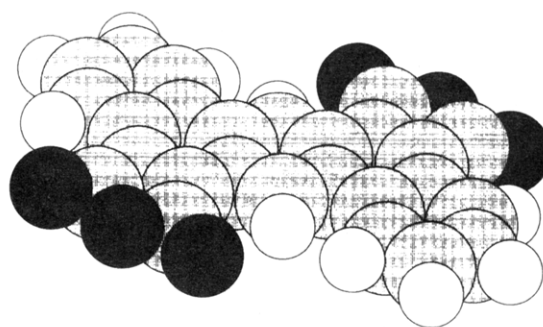
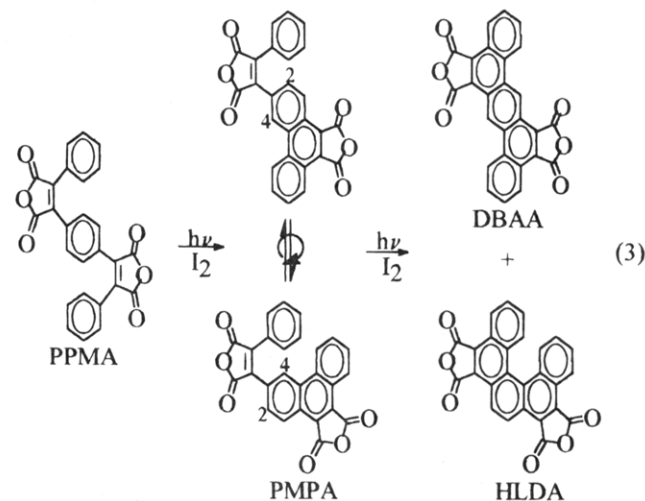


Figure 1. HyperChem space-filling model of DBAA.

(eq 3),^{20,21} and have also isolated a small amount (<5%)



of isomeric material. The HRMS and elemental analysis of both isomers correspond to a molecular formula of $C_{26}H_{10}O_6$, indicating that a double cyclization has occurred in both cases. Partial irradiation permits the isolation of the monocyclization intermediate 3-(phenylmaleic anhydride)phenanthrene-9,10-dicarboxylic anhydride [PMPA], which under the photolysis conditions generates the observed dicyclization products (eq 3).

The formation of two dicyclization isomers presumably results from the closure of the *ortho* carbon of the PMPA phenyl with either the C-2 or C-4 of the PMPA phenanthrene (eq 3). In the former case, the aforementioned flat and rigid dibenzanthracene system (DBAA) is formed. In the latter instance, however, a five-ring *ortho*-bonded helical structure results; hence, the name [5]helicene dianhydride (HLDA; see also eq 1). Although helicenes^{19,22} are well known, no dianhydrides have yet been reported. Molecular modeling studies²³ (Figure 2) predict HLDA to be helical in structure and twisted out of planarity because of the H-1/H-14 steric interaction (see eq 1). The helicene structure is, furthermore, predicted to be about 10 kcal/mol less stable than the isomeric DBAA.

(20) Liu, L.; B. Yang; Katz, T. J.; Pointdexter, M. K. *J. Org. Chem.* **1991**, *56*, 3769–3775.

(21) Liu, L.; Katz, T. J. *Tetrahedron Lett.* **1991**, *32*, 6831–6834.

(22) (a) Laarhoven, W. H.; Prinsen, W. J. C. *Top. Curr. Chem.* **1984**, *125* (Stereochemistry), 63–130. (b) Martin, R. H. *Angew. Chem., Int. Ed Engl.* **1974**, *13*, 649–660. (c) The numbering of the helicene carbons follows the convention first proposed: Newman, M. S.; Lednicer, D. *J. Am. Chem. Soc.* **1956**, *78*, 4765–4770. (d) Kuroda, R. *J. Chem. Soc., Perkin Trans. 2* **1982**, 789–794.

(23) The calculated heat of formation of the geometry optimized HLDA (Figure 2) is -70.936 kcal/mol (gradient 0.042 kcal/mol/Å). This should be compared to a value of $+1725.920$ (gradient 484.489) for the completely flat analog.

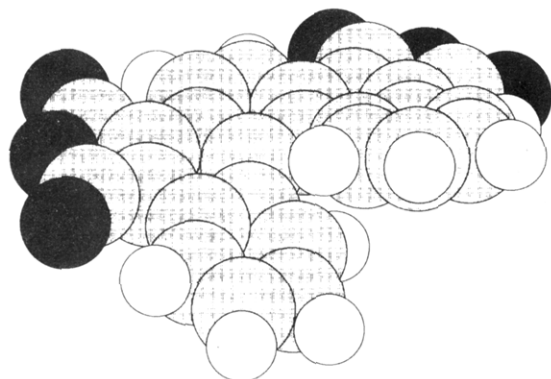


Figure 2. HyperChem space-filling model of HLDA.

Table 1. Selected Physical Data on HLDA Precursors and Isomers

	PPMA	PMPA	HLDA (major)	DBAA (minor)
DSC ^a	261	312	403 ^b	496 °C
FTIR (C=O)	1830	1841	1840	1842 cm ⁻¹ 1819 cm ⁻¹
NMR ^c (C=O)	1765	1770	1769	1755 cm ⁻¹ 164 ppm
MS (M ⁺)	164	164	163	164 ppm 418 amu

^a N₂ 200 psi. Modulated DSC confirms that the corresponding melt endotherms are reversible. ^b The mp determined by TMA on a pressed pellet was 400 °C. ^c For the purpose of comparison, the solid state ¹³C NMR carbonyl absorptions of 2,3-diphenylmaleic anhydride (DPMA, Aldrich) and the corresponding photocyclized analog, phenanthrene anhydride (PA, see experimental) are 164.74 and 160.31, respectively.

B. Identification and Characterization of HLDA and DBAA. The question remains: which is the major isomer, HLDA or DBAA? Fields *et al.*¹⁵ reports observing only one isomer and identified it as DBAA. His suggestion is based on his expectation that HLDA should show a large [M - 2C₂O₃ - H₂] peak as a result of a facile loss of the two anhydride moieties followed by further cyclization between C-1 and C-14. However, in our hands both isomers have [M - 2C₂O₃ - H₂] peaks with an amplitude of 1/4 of the [M - 2C₂O₃] peak.

As Table 1 reveals, the remaining spectral data as well as of little assistance in answering this question. Since both isomers are insoluble in most organic solvents, typical NMR characterization was precluded. Solid state ¹³C NMR was performed revealing in both cases three groups of broad absorptions: carbonyl (170–160 ppm), quaternary aromatic (130–140 ppm), and CH aromatic (120–130 ppm) (see Figure 3). Although there are indeed differences in the spectra of the two isomers (see Figure 3 and Table 1), each could well correspond to either structure. The melting points of both isomers are above 400 °C and were measured by differential scanning calorimetry (DSC). The lower melting point of the major isomer argues in favor of it being the less compactly packed HLDA, while the greater stability of DBAA might suggest that it is the major product. In short, the aforementioned data were not the type on which a solid characterization could be based.

(24) Surprisingly, however, the DSC-determined onset of melting for the crystalline samples is about 8–10 °C lower than the amorphous analog, though the maxima remain unchanged. Similarly, the TGA-determined *T_d* (onset) of the crystalline DBAA is as much as 70 °C lower than the corresponding amorphous analog (see the Experimental Section). TGA, DSC, or FTIR (interactive subtraction) of the recrystallized HLDA gave no indication of the presence of residual NMP. These results require further elucidation.

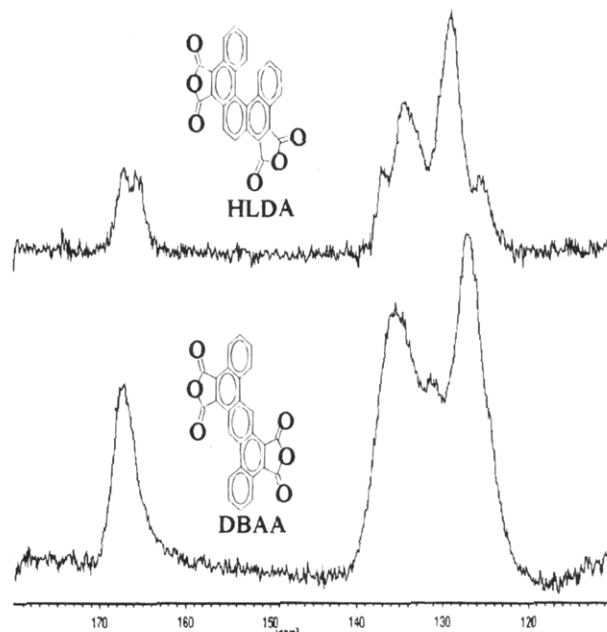


Figure 3. Solid state ¹³C NMR spectra of HLDA and DBAA.

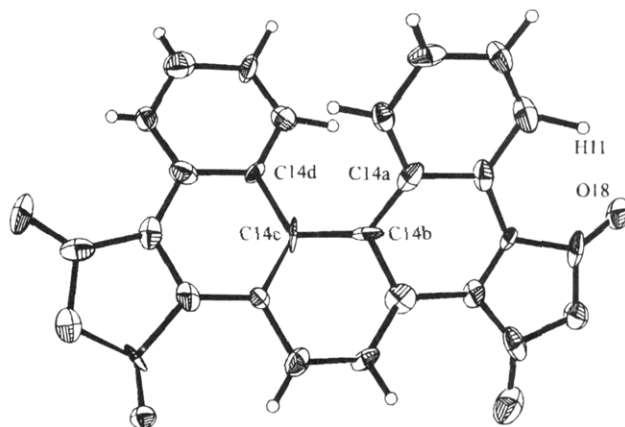


Figure 4. Thermal ellipsoid labeling diagram of HLDA. (The thermal ellipsoids were drawn at the 50% level.)

We did discover that the major isomer could be recrystallized from hot *N*-methylpyrrolidone (NMP) as yellow cubes.²⁴ X-ray crystallography easily supplied the desired information, demonstrating conclusively that the major isomer was HLDA. The crystal structure showing the thermal ellipsoids is given in Figure 4. The torsional angle defined by carbons 14a–14d is 32.8° (Figure 5). This is a bit larger than the value of 30° that Kuroda found for [5]helicene.^{22d} The distances (in Å) between a carbonyl oxygen and the closest aromatic hydrogen are as follows: O₁₈–H₁₁ = 2.243, O₁₅–H₄ = 2.793, O₁₆–H₇ = 2.501, O₁₇–H₈ = 2.510 or an average distance of 2.512 Å. These distances are not particularly short, and hence, we need not expect these hydrogens to effect a steric inhibition to anhydride opening of the type predicted for DBAA. Analysis of the packing diagram for HLDA revealed three short intermolecular hydrogen bonding interactions (Figure 6).

The preferential formation of HLDA is consistent with an earlier report of Laarhoven²⁵ that *p*-distyrylbenzene photocyclizes to 3-styrylphenanthrene (eq 4). Further

(25) Laarhoven, W. H.; Cuppen, Th. J. H. M.; Nivard, R. J. F. *Tetrahedron* **1970**, *26*, 1069–1083.

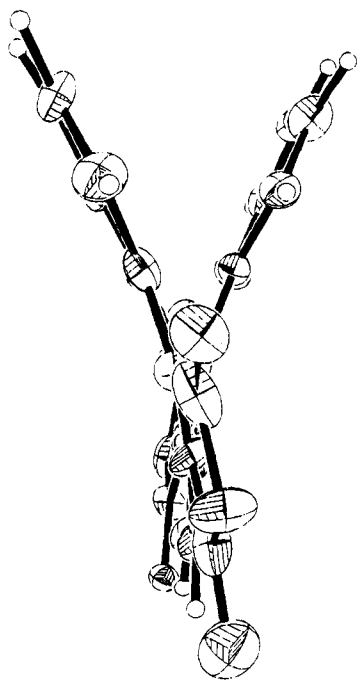
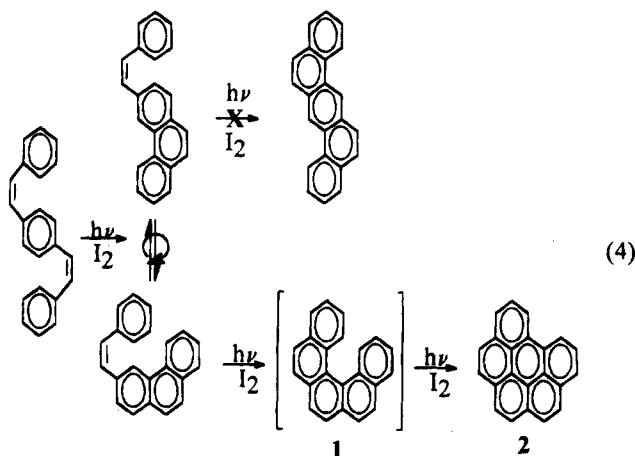


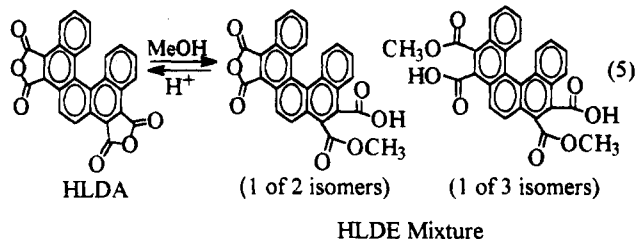
Figure 5. Diagram showing the torsional angle in HLDA.



cyclization of the latter could theoretically yield either [5]helicene (1) or dibenzanthracene. In fact, only a single product is observed which was identified as benzo[*cde*]perylene 2 and which is the known photodehydrocyclization product of 1.²⁶ The reason for the preferential formation of [5]helicene (1) has been rationalized in terms of a series of selection rules.^{22,25,26a,27} An extensive theoretical study is currently underway to determine their applicability to the PPMA to HLDA transformation as well, and in particular the effect of the anhydride moieties on the molecular orbital system.

C. Methanolysis of HLDA and DBAA. When crude HLDA (containing <5% DBAA) from the photolysis was suspended in refluxing methanol (ca. 0.1 M) for 1 week, approximately 40% of the dianhydride dissolved. More dissolved if the initial methanol to HLDA ratio was

larger. The resulting orange-yellow solution was filtered, and the undissolved precipitate proved to be HLDA substantially enriched in DBAA. (Indeed, repeated methanolysis of this sample ultimately yielded *pure DBAA*.) Evaporation of the filtrate gave a yellow solid which, unlike HLDA, was soluble in acetone and CHCl_3 . [Interestingly, the CHCl_3 solutions slowly (within 1 h) precipitated *pure HLDA*, undoubtedly by acid-mediated recyclization.] The mass spectrum of the yellow solid was essentially the same as that of HLDA, confirming the facile loss of methanol. The FTIR spectrum too was similar to that of HLDA but contained extra distinctive peaks at 3453 (br, s, acid OH), 1729 (s, acid C=O), and 1444 (m, acid COH bending). The ^1H NMR spectrum was quite complicated in the aromatic region but revealed methoxy peaks at 4.06, 4.08, and 4.10 ppm. The ^{13}C NMR was equally complicated but clearly indicated the presence of several sets of carbonyls at ca. 163 (anhydride), 168 (ester), and 171 (acid) ppm and methoxy carbons at ca. 53 ppm. While we cannot make a definite identification of the components of the product mixture, the chemical and physical data strongly support the suggestion that the mixture is comprised of the various isomers resulting from the methanolysis of one (two isomers) or both (three isomers) of the anhydrides of HLDA (see eq 5).²⁸ We will refer to this mixture of HLDA acid esters as HLDE.



The fact that DBAA, in contradistinction to HLDA, is totally resistant to methanolysis, lends credence to the correctness of the opening hypothesis of this paper. Namely, that the scission of the O-CO bond (be it solvolytic or thermal) in this polyaromatic compound is strongly inhibited by the 1,6-interaction between the H-4, H-7, H-11, and H-14 aromatic hydrogens (eq 1). The role of such steric pressure in stabilizing polyimides will be explored in future work.

D. [5]Helicene Photochemistry. Perhaps the most intriguing result is that HLDA, in contrast to the corresponding [5]helicene (1, eq 4),^{19,20} was not photocyclized further under the reaction conditions to the corresponding benzo[*ghi*]perylene 3 (eq 6). Such a lack of reactivity is not unprecedented, since hydrocarbons 4^{27d} and 6,²⁹ for example, also fail to undergo oxidative photocyclization (eqs 7 and 8).

The explanation given for the differing behaviors of 4 and 6 as compared to 1 relates to the fact that, in the first step of such photocyclizations, a HOMO to LUMO excitation occurs. Focusing on the coefficients of the two interior carbons, closure will be encouraged upon irradiation if the LUMO has greater bonding character than the corresponding HOMO.^{22,27d,29} Indeed, AM1 semiempirical

(26) (a) Scholtz, M.; Muhlstadt, M.; Dietz, F. *Tetrahedron* **1968**, 6845-6849. (b) See also refs 19 and 20.

(27) (a) Laarhoven, W. H.; Cuppen, Th. J. H. M.; Nivard, R. J. F. *Rec. Trav. Chim. Pays-Bas* **1968**, 87, 687-698. (b) Laarhoven, W. H.; Cuppen, Th. J. H. M.; Nivard, R. J. F. *Tetrahedron* **1970**, 26, 4865-4881. (c) Laarhoven, W. H.; Cuppen, Th. J. H. M.; Nivard, R. J. F. *Tetrahedron* **1970**, 26, 1069-1083. (d) Tinnemans, A. H. A.; Laarhoven, W. H.; Sharafi-Ozeri, S.; Muszkat, K. A. *Rec. Trav. Chim. Pays-Bas* **1975**, 94, 239-243.

(28) Mass spectral data suggests that at very long reflux times (~30 d) a diester anhydride and a tetraester are the primary products.

(29) Mallory, F. B.; Mallory, C. W. Unpublished results cited in ref 19, p 20.

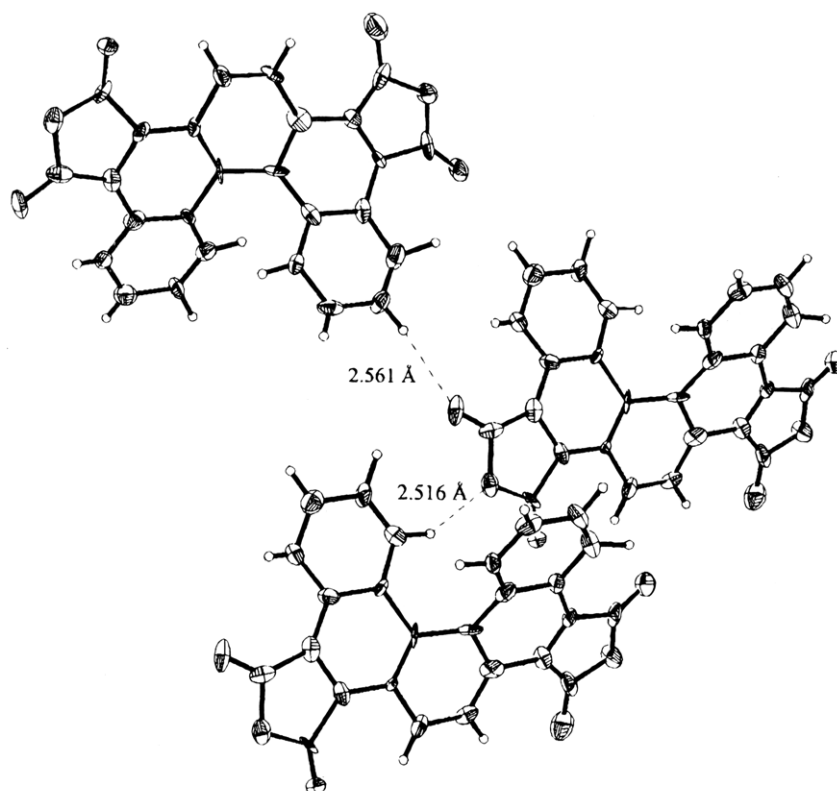


Figure 6. Packing diagram of HLDA showing the intermolecular hydrogen bonding interactions.

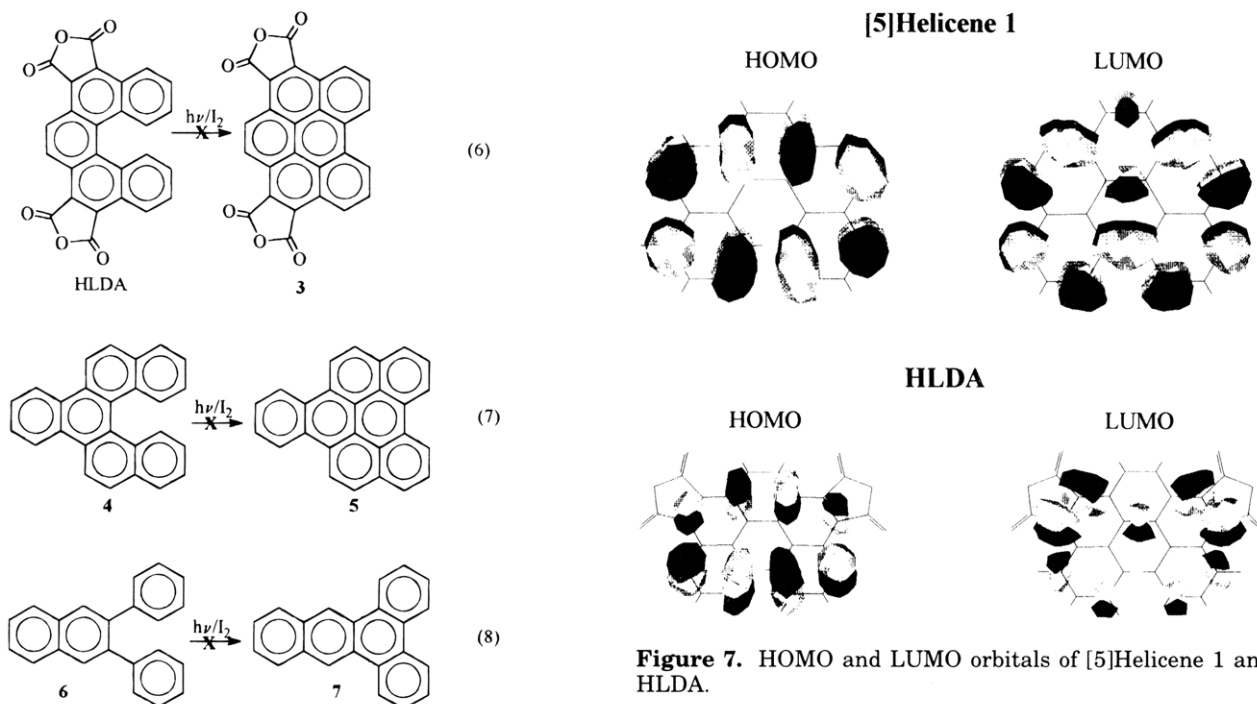


Figure 7. HOMO and LUMO orbitals of [5]Helicene 1 and HLDA.

calculations³⁰ predict that in the HOMO of both [5]-helicene (**1**) and HLDA there is an antibonding interaction between the two interior bonding carbons C-1 and C-14 (Figure 7). In the case of **1**, however, while the corresponding LUMO orbital has a sizable bonding interaction; there is no such interaction in the LUMO of HLDA.

(30) Autodesk HyperChem 3, AM1 semiempirical calculations of the orbitals were carried out on flat (non-geometry optimized) models of [5]helicene and HLDA. The molecular orbitals were drawn using Hypercube ChemPlus (Waterloo, Ontario).

Experimental Section

¹H and ¹³C NMR spectra were obtained on a Bruker AM 300 Fourier transform spectrometer. Solutions were generally prepared in CDCl₃ using TMS as the internal standard. Solid samples were run with a high power solid attachment using a side band suppression subroutine for cross-polarization. The solids probe was equipped with a dual air bearing capable of "magic angle" spinning at rates up to 5 kHz and tunable over the frequency range from ¹⁴N to ⁶³Cu. The solids spectra were externally referenced to the carbonyl of glycine (196.1 ppm relative to TMS). All IR spectra were recorded on KBr pellets using a Perkin-Elmer 1750 FTIR. Mass spectral analyses were performed by The Midwest Center for Mass Spectrometry

(Lincoln, NE) using a Kratos MS-50 triple analyzer. Elemental Analyses were performed by Spang Microanalytical Laboratory (Eagle Harbor, MI). Thin layer chromatography (TLC) was carried out on Merck silica gel F₂₅₄ precoated plates. Flash chromatography was performed on Merck silica gel, grade 60, 230–400 mesh, 60 Å. Melting points were determined in a Thomas Hoover capillary melting point apparatus and are uncorrected. Thermogravimetric analyses (TGA) were done on cured resin samples with a Perkin-Elmer TGS-2 (under air with a scan rate of 10 °C/min) using a PL Thermal Sciences (formerly Omnitherm Advantage II) thermal analysis system (TAS). Thermomechanical analyses (TMA) were carried out on cured resin samples with a DuPont Instruments 943 TMA (under air with a scan rate of 10 °C/min) using a PL Thermal Sciences TAS. Differential scanning calorimetry (DSC) was carried out on high melting monomer or imidized molding powder (prepolymer) in a Perkin-Elmer DSC 7 cell (under air or 200 psi N₂; scan rate: 10 °C/min) with a Perkin-Elmer Series 7 TAS. Modulated DSC analysis (for determining the reversibility of transitions) was performed with a Thermal Analysis Instrument (New Castle, DE) Module 2910 modulated DSC (N₂ purge; scan rate: 10 °C/min).

1,4-Phenylene Bis(phenylmaleic anhydride) [PPMA].

PPMA was prepared essentially as described by Fields *et al.*^{13–15} from 1,4-phenylenediacetic acid (Aldrich, 145.6 g, 0.75 mol) and sodium benzoate (Aldrich, 258.2 g, 1.5 mol) in 1 L of glacial acetic acid (Fisher) with the following modification of the workup and recrystallization procedure. After 1 h at reflux, the cooled solution was poured into 6 L of water,^{13,14} filtered, washed with water, and air dried overnight giving 356 g of brown powder. The crude product was washed four times with cold acetone yielding 3.5 L of a deep brown solution, which upon concentration gave 72 g of impure gold-brown powder (mp 253–255 °C). The remaining undissolved product (approximately 200 g of gold-brown powder) was then heated with 3.5 L of hot acetone yielding a green solution, which upon concentration gave 76 g of semipure brownish gold crystals (mp 260–261 °C). The remaining undissolved lemon-yellow product was dissolved completely in 6 L of hot acetone, which upon concentration gave 107 g of pure fluorescent shiny lemon-yellow platelets (mp 261–262 °C) (ca. 80% yield). We should note that recrystallization of the first two brownish gold fractions yielded purer product of higher mp (up to 261–262 °C) and crystallinity, but despite treatment with charcoal, the brownish-tint remained. PPMA is soluble in acetone, THF, and DMSO,¹⁵ as well as in CHCl₃, dioxane, and NMP.

PPMA: ¹H NMR (CDCl₃) δ 7.61 (bs, 4H, phenylene), 7.57–7.37 (m, 10H, phenyl); ¹³C NMR (CDCl₃) δ 164.391, 164.321, 139.608, 136.568, 131.670, 130.195, 129.773, 129.729, 129.156; ¹³C NMR (solid) δ 163.58 (CO), 138.59, 135.06, 129.87, 127.93; FTIR (KBr) 1830 (C=O, m), 1765 (C=O, s) cm⁻¹.

Photooxidative Cyclization of PPMA. Formation of HLDA, DBAA, and PMPA. PPMA was photocyclized by modifications of two literature methods: (a) Fields Method,^{13–15} A 3 L conical photochemical reactor fitted with a water-jacketed immersion well (containing a 450-W medium-pressure mercury vapor lamp surrounded by a Pyrex filter), a gas inlet tube, and a condenser (leading to a bubbler) was charged with PPMA (50.64 g, 0.12 mol), I₂ (0.24 g, 0.96 mol), and 2.8 L of acetone. The red-brown reaction mixture was magnetically stirred and irradiated under bubbling oxygen. The dull orange-yellow product, which is insoluble in the reaction solvent, tends to coat the immersion well, but can be removed as necessary with a Teflon spatula. The reaction mixture was filtered after 21, 42, and 111 h of irradiation yielding 7.38, 4.90, and 4.10 g, for a total of 16.38 g (0.039 mol, 33% yield) of product. A new portion of I₂ (0.24 g) was added to the reaction solution after each filtration. These first three fractions were identified by their IR spectral data as HLDA of varying purity, containing small (ca. 0–3%) but increasing amounts of DBAA. Further irradiation for an additional 87 h (while adding iodine every 24 h), yielded another 0.56 g (0.0013 mol, 1.1% yield) of a spectrally different product, subsequently identified as DBAA. A pure sample of DBAA was also obtained from repeated methanolysis of the above HLDA fractions (*vide infra*).

(b) Katz Method.²⁰ The aforementioned 3 L photochemical reactor was charged with PPMA (21 g, 0.05 mol), I₂ (26 g; 0.1 mol), 1.4 L of acetone, and 1.4 L of propylene oxide. The red-brown reaction mixture was flushed with N₂ for 20 min and irradiated under bubbling N₂. Product formed rapidly, and the immersion well had to be cleaned sometimes as often as every 1.5–2 h. After about 10 h of irradiation, the reaction solution had turned green (no I₂ remaining), product formation had essentially ceased, and the product formed had a dull yellow color. (On the basis of DSC data, the latter is primarily PMPA. Indeed, pure PMPA can be obtained by filtering the reaction solution every few hours so that photocyclization does not go to completion.) An additional portion of I₂ (12.8 g) was added, and the irradiation was continued (ca. 20 h) until the immersion well remained free of product for 2 h. The product, which now has the orange-yellow HLDA color, was gravity filtered, washed several times with acetone, and dried overnight in a vacuum oven at 200 °C to give an 88% yield of HLDA (18.4 g; 0.044 mol). DBAA and HLDA are insoluble in acetone, pyridine, CHCl₃, ethanol, ether, dioxane, DMF, DMAC, and HOAc. HLDA, and to a much lesser extent DBAA, is partially soluble in hot NMP (*vide infra*).

Crude HLDA (1 g from photolysis, contaminated with a few percent of DBAA) was partially dissolved in hot NMP (40 mL). The deep black/brown-green solution was filtered and concentrated down to 13 mL. [IR and DSC indicated that the undissolved material was a mixture of DBAA and HLDA.] The filtrate was allowed to cool slowly, with the concomitant formation of small green crystals (0.42 g); under a microscope, the latter proved to be yellow cubes. The mother liquor was concentrated down to ca. 7 mL, and a second crop was obtained (0.19 g; total of 0.61 g). The crystals were washed with cold acetone and dried at 200 °C overnight and 3 h at 260 °C to remove any residual NMP. TGA, DSC, or FTIR (interactive subtraction) of the recrystallized HLDA gave no indication of the presence of residual NMP. By comparison, DBAA is sparingly soluble in NMP, and repeated attempts to recrystallize it from this solvent failed. Instead, a fine brown powder was obtained, which was identified by IR and DSC as DBAA.

The DSC trace of HLDA is highly dependent on the method of analysis. Under 200 psi of N₂ pressure (see Table 1), the melt endotherm [402.5 (onset), 410.2 (max) °C] is followed by an exotherm [418.6 (onset), 445.6 (max) °C]. On the other hand, when the DSC is modulated³¹ and measured under N₂ purge (30 cm³/min), one observes a reversible melt endotherm [394.7 (onset), 412.9 (max) °C] accompanied by a second overlapping nonreversible endotherm [399.5 (onset), 426.1 (max) °C]. Furthermore, during the latter measurement, sublimed HLDA collects on the lid of the DSC chamber. We interpret the above data as follows: at ca. 400 °C and ambient pressure, HLDA melts (reversible transition) and volatilizes (nonreversible sublimation); however, at 200 psi, volatilization is inhibited and the melt is followed at around 420 °C by the onset of decomposition. Similarly, modulated DSC under N₂ purge of DBAA reveals that the reversible melt endotherm [489.4 (onset), 510.9 (max) °C] is accompanied by a large irreversible volatilization endotherm [470.0 (onset), 509.8 (max) °C]; as before, during the measurement, sublimed HLDA collects on the lid of the DSC chamber.

HLDA (amorphous powder from photolysis): DSC (N₂ 200 psi) typically 402.6 (onset), 412.6 (endo, max) °C [though some samples have shown values as high as 409.8 (onset), 413.8 (endo, max)], 418.6 (onset), 445.6 (exo, max) °C; Modulated DSC (amorphous, N₂ purge, 30 cm³/min) *normal heat-flow* 394.7 (onset), 412.9 (endo, max), 426.1 (endo, max) °C, *nonreversible heat-flow* 399.5 (onset), 426.2 (endo, max) °C, *reversible heat-flow* 394.7 (onset), 412.9 (endo, max) °C; TMA (pressed pellet, static air) 399.55 °C; TGA: T_d = 495.5 °C; mp

(31) Modulated or oscillating DSC is a new technique which permits the determination of reversible and nonreversible transitions. For recent references, see: (a) Reading, M.; Elliott, D.; Hill, V. L. *J. Therm. Anal.* **1993**, *40*, 949–955. (b) Cesaro, A.; Navarini, L.; Pepi, R. *Thermochim. Acta* **1993**, *227*, 157–166. (c) Reading, M. *Trends Polym. Sci.* **1993**, *1*, 248–253. (d) Sauerbrunn, S. R.; Crowe, B. S.; Reading, M. *Polym. Mater. Sci.* **1993**, *68*, 269–271. (e) Sichina, W. *J. Am. Lab.* **1993**, *25*, 26–30.

(TMA, static air) 399.6 °C; ^{13}C NMR (solid) δ 162.74 (C=O), 161.17 (C=O), 132.04, 130.22, 129.03 and 125.30 (aromatic); FTIR (KBr, %T) 1840.3 (C=O, 56), 1769.0 (C=O, 33), 1255.8 (82), 1196.0 (62), 1176.7 (82), 1163.2 (67), 1151.7 (78), 906.6 (70), 798.6 (78), 777.4 (81), 736.9 (90) cm^{-1} ; HRMS calcd ($\text{C}_{26}\text{H}_{10}\text{O}_6$, M^+) 418.0477, obsd 418.0489 (16.02); calcd ($\text{C}_{23}\text{H}_{10}\text{O}_3$, $\text{M} - \text{C}_2\text{O}_3$) 346.0629, obsd 346.0630 (13.67); calcd ($\text{C}_{22}\text{H}_{10}$, $\text{M} - 2\text{C}_2\text{O}_3$) 274.0782, obsd 274.0782 (16.29), calcd (C_{22}H_8 , $\text{M} - 2\text{C}_2\text{O}_3 - 2\text{H}$) 272.0626, obsd 274.0624 (4.69). Anal. Calcd ($\text{C}_{26}\text{H}_{10}\text{O}_6$): C, 74.64, H, 2.41. Found: C, 74.74; H, 2.51.

HLDA (after NMP recrystallization): DSC (N_2 200 psi) 393.9 (onset), 406.1 (endo, max), 411.6 (onset), 440.6 (exo, max) °C; Modulated DSC (N_2 purge, 30 cm^3/min) normal heat-flow 389.2 (onset), 412.1 (endo, max), 428.3 (endo, max) °C, nonreversible heat-flow 394.2 (onset), 429.9 (endo, max) °C, reversible heat-flow 385.1 (onset), 412.0 (endo, max) °C; TGA: $T_d = 422.5$ °C with second inflection at 489 °C.

DBAA: DSC (N_2 200 psi) 496.4 (onset), 506.1 (endo, max) 527.3 (endo, max) °C; Modulated DSC (N_2 purge, 30 cm^3/min) normal heat-flow 468.0 (onset), 509.6 (endo, max) °C, nonreversible heat-flow 470.0 (onset), 509.8 (endo, max) °C, reversible heat-flow 489.4 (onset), 510.9 (endo, max), 519.29 (endo, max) °C; ^{13}C NMR (solid) δ 163.50 (C=O), 132.02 (aromatic), 122.98 (aromatic); FTIR (KBr, %T) 1842.5 (43), 1819.10 (58) and 1755.45 (C=O, 60), 1257.75 (58), 1184.44 (33), 1167.08 (40), 910.52 (41), 781.27 (48) cm^{-1} ; HRMS: calcd ($\text{C}_{26}\text{H}_{10}\text{O}_6$, M^+) 418.0477, obsd 418.0469 (100); calcd ($\text{C}_{23}\text{H}_{10}\text{O}_3$, $\text{M} - \text{C}_2\text{O}_3$) 346.0629, obsd 346.0626 (49.01); calcd ($\text{C}_{22}\text{H}_{10}$, $\text{M} - 2\text{C}_2\text{O}_3$) 274.0782, obsd 274.0779 (36.82); calcd (C_{22}H_8 , $\text{M} - 2\text{C}_2\text{O}_3 - 2\text{H}$) 272.0626, obsd 274.0621 (9.81). Anal. Calcd ($\text{C}_{26}\text{H}_{10}\text{O}_6$): C, 74.64; H, 2.41. Found: C, 75.04; H, 2.40.

PMPA: mp (DSC, N_2 200 psi) 312.1 (onset), 315.8 (max) °C; ^{13}C NMR (solid) δ 163.87 (CO), 131.5 (aromatic), 125.89 (aromatic); FTIR (KBr, %T) 1841 (C=O, 17), 1770 (C=O, 3), 1627 (conjugated C=C, 42.8), 1256 (37), 1195 (17), 1176 (36), 1163 (20), 1151 (33), 907 (20), 800 (25), 779 (24) cm^{-1} ; HRMS calcd ($\text{C}_{26}\text{H}_{12}\text{O}_6$, M^+) 420.0634, obsd 420.0647. MS (EI, 70 eV, 300 °C) m/e 420 (M^+ , 100), 348 ($\text{M} - \text{CO} - \text{CO}_2$, 81.90), 276 ($\text{M} - 2\text{C}_2\text{O}_3$, 85.20), 274 ($\text{M} - 2\text{C}_2\text{O}_3 - \text{H}_2$, 46.86).

Photooxidative Cyclization of Diphenylmaleic Anhydride (DPMA). Formation of Phenanthrene-9,10-dicarboxylic Anhydride (PDA). Following the Katz method,²⁰ a 500 mL photochemical reactor (see previous section) was charged with DPMA (Aldrich, 5 g, 20 mmol), I_2 (5 g, 39 mmol), acetone (250 mL), and propylene oxide (250 mL). The reactor was flushed for 20 min with N_2 prior to irradiating the reaction mixture with a 450-W Hanovia lamp. After 2.5 h, the I_2 color had disappeared and substantial precipitate formed. (In contradistinction to the above photolysis of PPMA, no solid attached itself to the immersion well.) Additional I_2 (2 g) was added and the irradiation continued for another 1.5 h. The precipitate was filtered, washed three times with acetone, and dried in a 90 °C vacuum oven to give 3.85 g (15.5 mmol, 78% yield) of PDA. The IR, UV, and ^1H NMR spectra (DMSO 140 °C) have been reported.³²⁻³⁴

DPMA: ^{13}C NMR (solid) δ 164.74 (C=O), 137.83, 130.05 and 126.37 (aromatic).

PDA: mp (DSC, static air) 316.89 (onset), 318.01 (max) (lit.³⁵ mp 317 °C); ^{13}C NMR (solid) δ 160.35 (C=O), 132.10, 131.10, 125.20 and 124.41 (aromatic).

Methanolysis of HLDA. HLDE. HLDA (7.8 g, 18.6 mmol) was suspended in 180 mL of methanol and refluxed for 7 d. The resulting orange-yellow solution was filtered, and

Table 2. Crystallographic Data for HLDA

emp form	$\text{C}_{52}\text{H}_{20}\text{O}_{12}$
color; habit	yellow, cubes
form wt	836.7
cryst syst	monoclinic
space grp	<i>Cc</i>
cryst size (mm)	0.4 × 0.4 × 0.4
cell constants	
<i>a</i> (Å)	15.860 (3)
<i>b</i> (Å)	9.098 (2)
<i>c</i> (Å)	12.228 (2)
β (deg)	101.05 (3)
<i>V</i> (Å) ³	1731.8 (6)
<i>Z</i>	2
density (calcd) (g/cm^3)	1.604
absorp. coeff. (mm^{-1})	0.108
<i>F</i> (000)	856
temperature (K)	131
2θ range	3.5 to 45.0°
scan type	ω
scan speed (deg/min)	8.00
scan range (deg)	0.80(ω)
no. of reflns colld	1498
no. of indep reflns	1311
<i>R</i> _{int} %	0.95
no. obsd refl, $F > 2\sigma(F)$	1115
<i>R</i> (<i>F</i>)%	3.29
<i>R</i> _w (<i>F</i>)%	3.96
GOF	1.11

the undissolved precipitate (4.7 g, 11.2 mmol; 40% dissolved) proved to be HLDA substantially enriched in DBAA. (Repeated methanolysis of this sample ultimately yielded pure DBAA.) Rotary evaporation of the filtrate yielded a yellow solid. The latter was identified as a mixture of the isomers of the monoanhydride acid ester of HLDA and the diacid diesters (HLDE).

HLDE: ^1H NMR (CDCl_3) δ 9.0–8.6, 8.4–8.2, 8.2–7.9 and 7.9–6.9 (overlapping m, aryl), 4.10, 4.08 and 4.06 (CH_3O); ^{13}C NMR (CDCl_3) δ 171.82, 171.69 and 171.23 (acid C=O), 168.39, 168.12 and 163.29 (ester C=O), 163.23, 163.02 and 162.72 (anhydride C=O) [multitude of aromatic peaks of the various isomers deleted] 53.47, 53.41, 53.34 and 53.29 (CH_3O); FTIR (KBr, %T) 3453 (br, 25), 1843 (C=O, 21), 1768 (C=O, 33), 1729 (10), 1444 (35), 1260 (20), 1197 (13), 1176 (33), 1166 (34), 1154 (36), 912 (36), 798 (38), 766 (36) cm^{-1} ; MS (EI) m/e 418 (6.29), 346 (39.26), 274 (100), 272 (36.95).

Crystallographic Analysis. Crystals of HLDA were grown from slow concentration of a NMP solution. A yellow crystal measuring 0.4 × 0.4 × 0.4 was mounted on a glass fiber and aligned on a Syntex P2₁ diffractometer. Final unit cell parameters were determined by least square refinements of 25 reflections with $20^\circ < 2\theta < 30^\circ$. Crystal data, data collection and reduction, and structure refinement details are listed in Table 2. Crystal stability was monitored by measuring three standard reflections every 97 measurements. Data were corrected for Lorentz and polarization factors and reduced to unscaled *F* values. Crystallographic calculations were performed by using the Siemens SHELXTYLPLUS (PC Version)³⁶ program library. The position of all the atoms were determined by direct methods. All non-hydrogen atoms were refined anisotropically by use of full matrix least-squares methods. The hydrogen atoms were refined isotropically with the isotropic thermal parameters fixed at 0.05 Å². The final agreement factors for the 1311 data ($F > 2.0\sigma(F)$) were $R_f = 3.29$, $R_{wf} = 3.96$, and GOF = 1.11.

Acknowledgment. A.A.F. would like to acknowledge the kind and generous support of the National Research Council and NASA Lewis Research Center, in particular the warm hospitality of the Polymers Branch.

JO941976V

(32) Sargent, M. V.; Timmons, C. J. *J. Chem. Soc.* **1964**, Suppl. 1, 5544–5552.

(33) Matsuo, T.; Tanoue, Y.; Matsunaga, T. Nagatoshi, K. *Chem. Lett.* **1972**, 709–712.

(34) Hacker, N. P.; McOmie, J. F. W. *Tetrahedron* **1984**, *40*, 5249–5254.

(35) Hacker, N. P.; McOmie, J. F. W.; Meunir-Piret, J.; Van Meerssche, M. *J. Chem. Soc., Perkin Trans 1* **1982**, 19–23.

(36) Nicolet Instrument Corp., Madison, WI, 1988.